RSC Advances

ROYAL SOCIETY OF CHEMISTRY

www.rsc.org/advances

Journal Name

RSCPublishing

ARTICLE

Scalable preparation of nitrogen-enriched carbon microspheres for efficient CO_2 capture

Cite this: DOI: 10.1039/xoxxoooooox

Mei Wang[a], Jitong Wang[a], Wenming Qiao[a,b], Licheng Ling[a,b] and Donghui Long[a,b]*

Received ooth January 2012,
Accepted ooth January 2012

DOI: 10.1039/xoxxoooooox

www.rsc.org/

Monodispersed nitrogen-enriched carbon microspheres with uniform and tunable particle size and high nitrogen content were prepared by a simple carbonization of melamine-resorcinol-formaldehyde (MRF) microspheres. The MRF polymer microspheres were obtained by a hydrothermal polymerization at a temperature ranging from 80 to 180 °C and with a wide reactant concentration and a wide precursor composition. The synthesis is simple, scalable and very flexible, allowing the easy tailoring of the microsphere size and the nitrogen content in the carbon framework. The pores are created by the release of volatile matter during carbonization, giving a large fraction of fine micropores with BET specific surface area of 400-800 m^2/g. Further CO_2 activation can increase the BET surface area into 1500 to 1900 m^2/g. Depended on the precursor composition, the nitrogen-enriched carbon microspheres contain 0-22.5 wt. % of nitrogen atoms which are predominantly constituted by pyridinic-N, quaternary-N and oxynitride. CO_2 capture performances were evaluated between 273 K and 348 K, and very high adsorption capacity of 4.50 mmol/g at 273 K, 1 bar is achieved. The facile and environmental friendly production, scalable preparation, fast CO_2 adsorption kinetics and good regeneration performance make the prepared carbon microspheres be useful for practical applications.

1 Introduction

Significant research activities have been undertaken in recent years to prepare carbon microspheres with controllable pore structure,[1] because they have widespread applications in drug delivery,[2] active material encapsulation,[3] biodiagnostics,[4] catalyst supports,[5] lithium-ion battery electrodes,[6] electrochemical capacitors,[7] and gas adsorption[8-10] etc. Up to now, various methods have been developed for the synthesis of carbon microspheres. (i) Hydrothermal carbonization of carbohydrate sources, such as glucose,[11-13] sucrose,[14, 15] fructose,[16] cellulose,[17] starch,[18] which result in carbon microspheres with the size ranging from about 100 nm to micrometers. (ii) Pyrolysis of carbon precursors formed by emulsion polymerization, self-assembly, nanocasting approach and ultrasonic spray pyrolysis, which employ resorcinol-formaldehyde,[19] melamine-formaldehyde,[20] furfuryl alcohol[21] or phenol-melamine-formaldehyde[22] as organic precursors. (iii) Chemical vapor deposition (CVD) of hydrocarbons such as ethylene,[23] toluene,[24] mesitylene[25] and deoiled asphalt[26] on substrates, where carbon microspheres can be achieved via continued deposition and decomposition of gaseous carbon precursor. (iv) Extension of the Stöber method, using the ammonia as catalyst in alcohol/water solution to prepare phenolic resin microspheres and carbon microspheres, which possess covalently bonded three-dimensional (3D) frameworks, high uniformity and tunable size.[27, 28] All of these methods lead to various carbon microspheres, although regulating the morphology could be successfully demonstrated. As for the potential application of a newly developed material, the production at large scale with low cost is the last bottleneck. It is highly essential to explore economical and high-throughput methods for the synthesis of carbon microspheres with uniform sphere sizes, and high specific surface area for various applications.

The properties of carbon microspheres depend to a large extent not only on the porosity but also on the heteroatoms that decorate their surface. By having the ability to control the chemical environment within the pores of microporous networks, it is able to tune a network's interactions with guest molecules, making them increasingly tailored for specific applications. Nitrogen atom is one of the most important and widely introduced heteroatoms which appear as amine-like surface functionalities, and more often directly doped into the backbone of the carbon. There has been growing evidence showing that nitrogen doped carbon materials are promising candidates for electric double layer capacitor (EDLC),[29] selective catalytic reduction [30] and gas adsorption[31-33] and so on.

Nitrogen doping endows the carbons with high electric conductivity and a polar nature, which is beneficial for electronic transmission and introduce basic functionalities enhancing the specific adsorbent-adsorbate interaction for acid molecules like CO_2. *Lu* and coworkers[34] prepared nitrogen-doped porous carbon monoliths by polymerization of resorcinol and formaldehyde catalysed by nitrogen-containing lysine. The results demonstrated that both nitrogen groups and the presence of micropores are necessary for achieving a high CO_2 capture performance, with a maximum up to 3.13 mmol/g. *Jin* and coworkers[35] prepared N-doped microporous carbons by chemical vapor deposition methods using zeolite NaY as a hard template and furfuryl alcohol/acetonitrile as carbon precursors. Their study suggested that low temperature vapor deposition of acetonitrile could introduce the basic nitrogen functionalities which increase the negative charge density and simultaneously increase the adsorption of CO_2. *Zhu* and coworker[36] prepared porous nitrogen-doped compound derived from the carbonization of an imidazolium-based ionic liquid, the basic sites within modified microporous carbon adsorbents display an exceptional CO_2 absorption capacity of 4.39 mmol/g at 0 ^oC and 1 bar. Higher CO_2 adsorption capacity can be achieved *via* KOH,[37-40] $ZnCl_2$[41,42] or CO_2[43,44] activation with one step or post treatment. Nevertheless, it remains a great challenge to place desired functionalities and to control over their amount within a carbon network at industrial scale for special applications.

Herein, we report an effective synthesis of nitrogen-enriched carbon microspheres with uniform and tunable particle size by direct carbonization of polymer microspheres, based on our previous work on the preparation of nitrogen-rich phenolic microspheres. The phenolic microspheres were prepared by a direct copolymerization of melamine, resorcinol and formaldehyde in water at a wide temperature range (80-180 ^oC) and a wide reactant concentration (5-20 %w/v). After a simple carbonization at 800 ^oC, the monodispersed carbon microspheres with controllable nitrogen content were obtained in this work. To the best of our knowledge, this is the first report on carbon microspheres by rationally introducing a very wide nitrogen content from 0 to 22.5 wt. %. Furthermore, the effectiveness of the nitrogen-enriched carbon microspheres as a CO_2 adsorbent was evaluated. The nitrogen-enriched carbon microspheres can be further treated by CO_2 activation to greatly improve the specific surface area, which may extend them into a more wide applications. The synthesis approach develops a low cost and environmental friendly route for making nitrogen-enriched carbon microspheres with controllable nitrogen content. The process is very facile and all of the precursors used in the process are commercially available, which will be suitable for scale-up production. This promises this kind of new nitrogen-enriched carbon microspheres with tailored physical and chemical properties for further industrial applications.

2 Experimental

2.1 Synthesis of the carbon microspheres

All chemicals were purchased from Titanchem Co. and used without further treatment. Previously, we have successfully prepared the melamine-resorcinol-formaldehyde polymer microspheres with controllable nitrogen contents and particle size.[45] The polymer microspheres were synthesized in water via a hydrothermal method using resorcinol (R) and formaldehyde (F) as the carbon source and melamine (M) as the nitrogen source. Typically, 3.87 g R and 5.70 g F (37 wt.%) were dissolved and stirred in 30 ml DI water for 2 h at 40 ^oC. Meanwhile, 4.43 g M and 8.56 g F (37 wt. %) were dissolved in 30 ml DI water and stirred at 80 ^oC until the solution became clear. After cooling down to 40 ^oC, the MF solution was added into the RF solution and stirred for 30 min. The mixed solution was then transferred to a closed bottle and heated at 80 ^oC for 24 h. After filtration, washing and air-dried at 100 ^oC for 24 h, the polymer microspheres were collected and denoted as MRF-x, where x represents the molar ratio of melamine to resorcinol (M/R). The carbon microspheres were formed after carbonization at 800 ^oC for 2 hours in N_2 flow, and denoted as MRFx-C. It is worth to mention that when M/R equals to 0 (no M), or R/M is 0 (no R), the resulting carbon microspheres were labeled as RF-C and MF-C, respectively for short.

The CO_2 activation for carbon microspheres was performed by placing a ceramic boat with 1 g of carbon microspheres in a ceramic tube furnace under flowing nitrogen with a heating rate of 10 °C/min up to 900 °C. After reaching this temperature, the activating gas was introduced for 3 h and then switched back to nitrogen to prevent further activation during the cooling process. The activated carbon microspheres were denoted as A-MRFx-C.

2.2 Characterization

The morphologies of the spheres were observed under scanning electron microscopy (SEM, JEOL 7100F). The microstructures were observed under transmission electron microscopy (TEM, JEOL 2100F) operated at 200 kV. Nitrogen adsorption/desorption isotherms were measured at 77 K with a Quadrasorb SI analyser. Before the measurements, the samples were degassed in vacuum at 473 K for 12 h. The Brunauer-Emmett-Teller (BET) method was utilized to calculate the specific surface areas (S_{BET}). The pore size distributions (PSDs) were determined from the quenched solid-state DFT model. The total pore volumes (V_{total}) were estimated from the amount adsorbed at the maximal relative pressure of 0.985. Micropore surface areas (S_{micro}) were obtained via t-plot method. The surface chemistry was obtained from an Axis Ultra DLD X-ray photoelectron spectroscopy. The X-ray source operated at 15 kV and 10 mA. The working pressure was lower than 2×10^{-8} Torr (1 Torr = 133.3 Pa). C1s, N1s and O1s XPS spectra were measured at 0.1 eV step size. N1s XPS signals were fitted with mixed Lorentzian-Gaussian curves, and a Shirley function was used to subtract the background. Elements analysis was used to determine the contents of carbon (C), hydrogen (H) and nitrogen (N) directly on Elemental Vario EL III using the thermal conductivity detector. The X-ray diffraction (XRD) patterns were acquired on a Rigaku D/max 2550 diffractometer

operating at 40 KV and 20 mA using Cu Kα radiation (λ = 1.5406 Å). Raman spectra were recorded with a Renishaw system 1000 with an argon-ion laser operating at 514 nm with a charged-coupling-device detector.

2.3 CO_2 capture measurements

The CO_2 adsorption isotherms of the as-prepared carbon microspheres were measured using a Quantachrome Quadrasord *SI* analyzer at different temperatures. In order to remove the impurities such as water and CO_2 adsorbed at room temperature, the samples were degassed in vacuum at 473K for 12 hours before measurements, and cooled down naturally.

CO_2 adsorption/desorption measurements were performed on a TA Instruments Q600 TGA/DSC thermogravimetric analyzer. Typically, about 10 mg of carbon microspheres was placed in an alumina sample pan. After the sorbent was heated to 100 °C in N_2 (100 ml/min) for 100 min to remove the moisture and CO_2 adsorbed from the air, the temperature was decreased to 25 °C. Then the feed gas was switched to CO_2 (100 mL/min) for 100 min for the adsorption study. The CO_2 capturing capacity of the sorbent was calculated from the weight gain of the sorbent during the adsorption process. For regenerability, the samples were pretreated in N_2 at 110 °C for 30 min, then exposed to CO_2 at 25 °C for 100 min. This process was repeated for 10 times.

3 Results and discussion

3.1 Characterizations

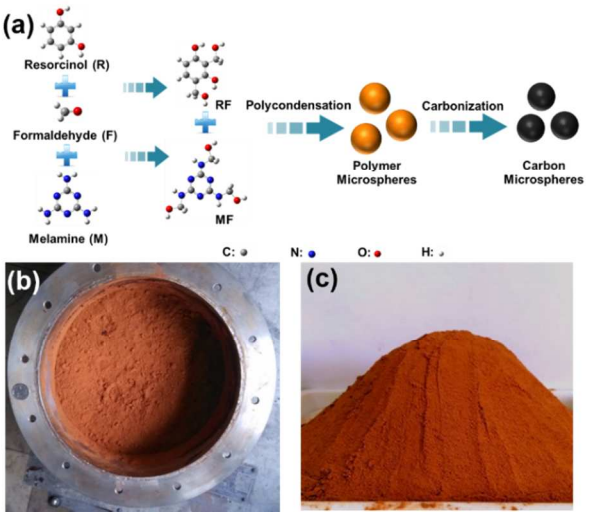

Fig. 1 Schematic illustration of the carbon microspheres preparation (a), scalable preparation of nitrogen-enriched polymer microspheres (b) and(c). (R/F=1:2, M/F=1:2, M/R=1:1, polymerization temperature: 80 °C, yield: 85%, size of the mould: Ø300*150 mm)

Fig. 1 illustrates the preparation of MRF polymer microspheres and the resulting carbon microspheres. As we previous reported, the co-condensation of MF and RF can successfully produce homogeneous MRF polymer microspheres without using any catalysts.[45] This process is believed to be similar to the Stöber process via a monomer addition in which nucleation is a fast process, followed by a particle growth process without further nucleation. The polymer MRF microspheres with tuneable particle size can be obtained at a wide temperature (80-180 °C) and a wide precursor composition (M/(R+M) = 0-1). Moreover, the reaction concentration (M+R+F) can achieve a very high level, such as 20%w/v (20 g polymer per 100 ml H_2O). That means we can produce 1 kg polymer microsphere in a 5 L vessel (see image in Fig. 1b and Fig. 1c). During the high temperature pyrolysis, the polymer microspheres convert into carbon microspheres, while partial nitrogen atoms could be inherited and incorporated into carbon framework. The total synthesis process is very simple and scalable, which have a great potential to be produced on an industrial scale.

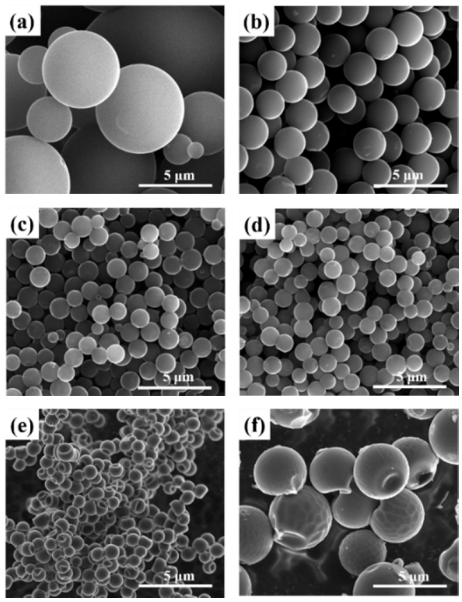

Fig. 2 SEM images (a-f) of RF-C (a), MRF1-C (b), MRF2-C (c), MRF3-C (d), MRF5-C (e) and MF-C (f).

Fig. 2 and Fig 3 show the typical SEM and TEM images of the obtained carbon microspheres with the different M/R ratios. It was found that the particle size of polymer microsphere could be adjusted from 12 μm to 1μm only by increasing the M/R ratio in the precursor composition (see Fig. S1). After carbonization, the carbon microspheres experience different extent shrinkage in diameter, and their morphologies and particle sizes largely depend on their precursor composition. As shown in Fig. 2, the direct hydrothermal polymerization of resorcinol-formaldehyde or melamine-formaldehyde without any additives could produce microspheres with relatively wide particle size distribution (0.5-8 μm).The addition of melamine into resorcinol-formaldehyde system could apparently decrease the particle size of the microspheres and improve the size uniformity. Here the melamine may play dual roles on the formation of smaller microspheres. On one hand, the melamine could sever as a basic catalyst to accelerate the polymerization of resorcinol-formaldehyde. On the other hand, melamine is a hexafunctional monomer while resorcinol is a trifunctional monomer, as polymerization proceeds, the cross-link density and molecular weight of polymers increases with increasing M/F ratios, which fast nucleation rates and decrease the time of growth stage. As a result, smaller polymer and carbon microspheres are formed at a higher M/R ratio. It should be noted higher ratio of melamine in the precursor (M/R=5 or MF)

could result in the formation of collapse structure in carbon microspheres, due to the high-level pyrolysis of melamine resin compared to the resorcinol-formaldehyde resin. TEM images as shown in Fig. 3 give clear observations of MRF3-C, which further confirms that the carbon microspheres have good spherical morphology.

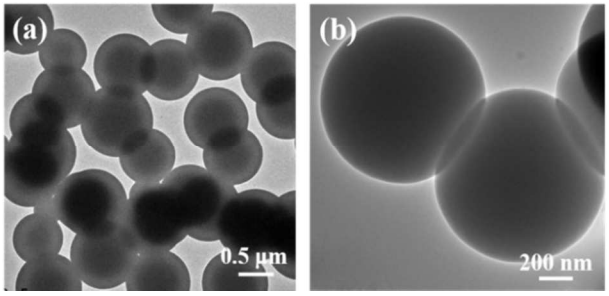

Fig. 3 TEM images of MRF3-C with different magnification

During the carbonization, the micropores are created by the release of volatile that is dependent on the precursor composition. Fig. 4 shows the N_2 adsorption-desorption isotherms and the resulting DFT pore size distributions of the carbon microspheres. All isotherms exhibit type I with a sharp increment at low relative pressure and a platform in high relative pressure range (0.2-1.0), which indicates the presence of considerable micropores. The detailed porosity parameters are summarized in Table 1. The specific surface areas (S_{BET}) and total pore volumes (V_{total}) for MRF-C samples are 596-796 m^2/g and 0.25-0.36 cm^3/g, respectively. The microporosity of the nitrogen-free carbon microspheres (RF-C) is relatively underdeveloped. The addition of melamine could increase the amount of the volatile compounds, thus creating more accessible microporosity inside the MRF-C network. Accordingly, the BET surface area and total pore volume generally increases with the M/R ratio and exhibit a maximum at the M/R of 3. However, further increasing the M/R ratio causes the obvious decrease of the S_{BET} and V_{total}, suggesting the inhibiting effect of excessive incorporated nitrogen on the formation of micropores during the pyrolysis. The pore size distributions (PSDs) calculated using the DFT model (Fig. 4b) show the carbon microspheres prepared with different M/R ratios have relatively narrow microporous size distribution centered at 0.6-0.7 nm. According to previous reports, the micropores smaller than 0.8 nm are responsible for the CO_2 capture,[46, 47] which makes the materials a suitable adsorbents.

The chemical compositions of these carbon microspheres were measured by elemental analysis, as listed in Table 2. The nitrogen content would be easily controlled in a wide range by changing the initial melamine content in the precursors. A higher initial molar ratio of M/R in the precursor leads to a higher N

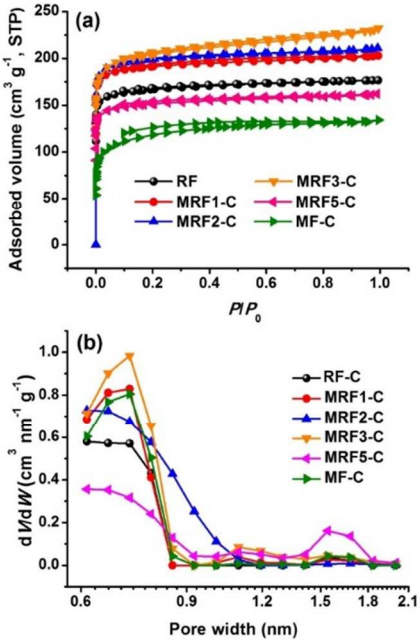

Fig. 4 N_2 adsorption isotherms at 77K (a) and pore size distributions (b) of as prepared carbon microspheres

Journal Name

RSCPublishing

ARTICLE

Table 1. Porosity parameters and CO2 adsorption capacity of the carbon microspheres

Samples	S_{BET}[a] (m^2/g)	S_{mic}[b] (m^2/g)	V_{total}[c] (cm^3/g)	V_{mic}[d] (cm^3/g)	D_P[e] (nm)	CO_2 adsorption capacity (mmol/g)	
						273 K	298 K
RF-C	658	616	0.27	0.25	0.61	3.91	2.90
MRF1-C	755	714	0.31	0.28	0.72	4.50	3.28
MRF2-C	785	741	0.33	0.30	0.61	4.39	3.29
MRF3-C	796	713	0.36	0.29	0.72	4.29	3.25
MRF5-C	596	561	0.25	0.22	0.72	3.47	2.60
MF-C	443	334	0.21	0.15	0.61	2.81	2.13

S_{BET}[a]: specific surface area; S_{mic}[b]: Micropore surface area; V_{total}[c]: total pore volume measuerd at P/P0= 0.99; V_{mic}[d]: micropore volume determined from the Dubinin-Radushkevic equation; D_p[e]: The maximum pore diameter of the PSDs calculated by the QSDFT method.

Table 2. Chemical composition of the carbon microspheres measured by elemental analysis and XPS techniques

Samples	Elements analysis				XPS analysis			
	N (wt.%)	C (wt.%)	O (wt.%)	N/C (at./at.)	N (wt.%)	C (wt.%)	O (wt.%)	N/C (at./at.)
RF-C	0	96.04	3.15	0	0	87.65	12.35	0
MRF1-C	7.36	79.11	12.02	0.08	18.58	68.24	13.18	0.27
MRF3-C	12.47	69.89	15.68	0.15	23.17	55.24	21.59	0.42
MRF5-C	19.10	71.78	7.97	0.27	32.31	50.40	17.29	0.64
MF-C	22.48	65.36	0.662	0.34	39.13	49.10	11.77	0.79

content in the polymeric microspheres (see Table S1), and therefore in the carbon microspheres (Table 2). In this work, we could adjust the nitrogen content from a very wide range of 0-22.5 wt%. Such high nitrogen content and wide adjustable extent in the carbon materials are rarely reported. High-resolution XPS was further employed to investigate the chemical composition and nitrogen bonding configurations formed in the surface of the carbon framework. The calculated nitrogen content is in the range of 18.5-39.1% by adjusting the M/R ratio, slightly higher than the corresponding value obtained from the elemental measurements. This can be explained by the surface specificity of XPS measurements, suggesting that the N atoms are apt to gather on the surface rather than the bulk body of carbon frameworks. The high-resolution C 1s spectra show a unimodal peak shape at 284.8 eV which is related to the graphitic carbon. The N1s spectra (Fig. 5c) are curve-fitted into three peaks with binding energies of 398.5 ± 0.3, 401.1 ± 0.3 eV and 403.6 ± 0.3 eV that corresponding to pyridinic N (N1), graphitic N (N3) and oxynitride, respectively. No pyrrolic N is resolved. The graphitic N is the dominant form representing around 45-55%, which might issue from the triazine ring of melamine. In addition, the relative atomic ratio of pyridinic N is obviously

increase with the M/P ratio, suggesting more nitrogen atoms are formed at the edges of graphitic layers.

The microcrystalline structures of the carbon microspheres with different nitrogen contents were characterized by XRD, as shown in Fig. 6a. All carbon microspheres show very similar diffraction features with two characteristic peaks at ca. 25.1° and 43.9°, corresponding to the reflections of the graphitic planes (002) and (100), respectively.[48] The positions of two peaks do not change with the nitrogen content. However, the intensity of the (100)-diffraction line, referring to the interlayer organization, decreases gradually with the nitrogen content increasing. The result suggests high nitrogen atom doping could break the unity of graphitic structure and decrease the size of graphitic structural units. The structural variation of the carbon microspheres was further demonstrated by Raman spectroscopy, as shown in Fig. 6b. The peak at 1350 cm^{-1}, signed as the D-band, is associated with the breathing mode of κ-point phonons of A_{1g} symmetry,

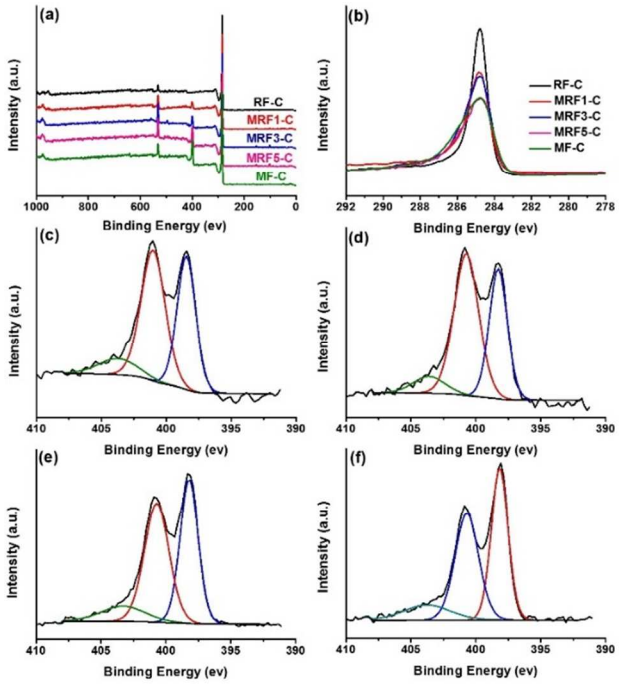

Fig. 5 XPS survey (a), high-resolution C 1s (b) and high-resolution N 1s (c-f) spectra of the carbon microspheres with different M/R ratios: MRF1-C (c), MRF3-C (d), MRF5-C (e) and MF-C (f).

whereas the G-band at 1581 cm^{-1}, is associated with E_{2g} mode for disordered graphitic materials.[49] There is no dependence of the position of the two bands on the nitrogen content. However, a continuous increase of the vibration frequency and the half-widths corresponding to the D line is observed with the increase of the nitrogen content in the carbon microspheres. Also, the intensity ratios of the D-band to the G-band (I_D/I_G) increases with the increase of nitrogen content, suggesting that the defectiveness of the graphite-like layers grows with increasing nitrogen content. Additionally to defects, this may be also due to the influence of the nitrogen doping spoiling the local symmetry. Therefore, from XRD and Raman results, it can be concluded that higher N doping tends to decrease the size of graphitic structural units and introduce more disorder in the graphitic structure.

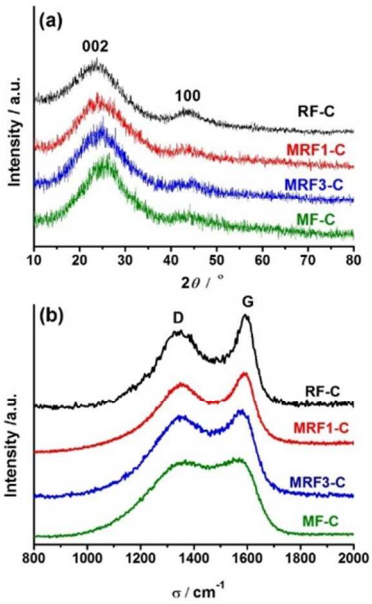

Fig. 6 XRD (a) and Raman (b) spectra of the carbon microspheres with different M/R ratios

3.2 CO_2 capture

It has been already reported that nitrogen doping can enhance the acidic CO_2 adsorption capability of carbon materials, but the relationship of nitrogen content with CO_2 adsorption is rarely revealed. Hence, it is interesting to estimate the CO_2 adsorption performance of these carbon microspheres with different nitrogen contents. Herein the CO_2 uptakes of the carbon microspheres were measured up to 1 bar at 273 and 298 K, as shown in Fig. 7. The nitrogen-free RF-C carbon microspheres have a CO_2-adsorption capacity of 3.90 mmol/g at 273 K and2.90 mmol/g at 298 K. By introducing the nitrogen content, MRF1-C exhibits significantly improved CO_2 adsorption capacity of 4.50 mmol/g at 273 K and 3.28 mmol/g at 298 K which should be attributed to the strong interaction between CO_2 molecular and basic amine groups and the fine micropores. These values are higher than those of many reported carbon materials without activation.[34, 35, 50-54] Further increase in nitrogen content has little effect on the CO_2-adsorption capacity, with MRF2-C and MRF3-C being similar to MRF1-C. However excess nitrogen doping (MRF5-C and MF-C) would lower down the adsorption capacity to only 2.14 mmol/g at 298 K and 2.81 mmol/g at 273 K. This is due to the decreased surface area compensated for by the increased nitrogen content. This study indicates the dominating role of surface area in CO_2 adsorption in relation to the effect of N%, which seems to be less pronounced at higher nitrogen content. The detailed CO_2 adsorption capacity data can be seen in Table 1.

To determine the strength of the interaction between CO_2 molecular and carbon microspheres, the isosteric heats of adsorption (Q_{st}) as a function of CO_2 adsorption capacity (Fig. 7 c) were calculated according to Clausius-Clapeyron equation:

$$\left(\frac{\partial(\ln P)}{\partial(1/T)}\right)_{q_a} = \frac{Q_{st}}{R}$$

where P is the partial pressure of CO_2 (Pa), T is the absolute temperature (K), R is planck constant, 8.314 $J \cdot mol^{-1} \cdot K^{-1}$. The Qst of the carbon microspheres decreases with the CO_2 capacity increases. The nitrogen doped carbon microspheres provide higher Q_{st} at low coverage than the nitrogen free sample, due to the favourable interactions between the adsorbed CO_2 molecules and the Lewis basic amine functionalities. However, at high relative pressure ranging from 0.4 to 1.0, the isotherms of the carbon microspheres are almost linear (Figure 7d.), which indicates that the interaction between CO_2 molecules and N-containing groups becomes weak at higher coverage, and physical adsorption derived from van der Waals interaction dominates the process. Therefore, the isosteric heats decreases at higher coverage. The average of the heat of adsorption for MRF1-C is 30.5 kJ/mol, approximately to that of activated carbon[55] and some MOFs materials.[56]

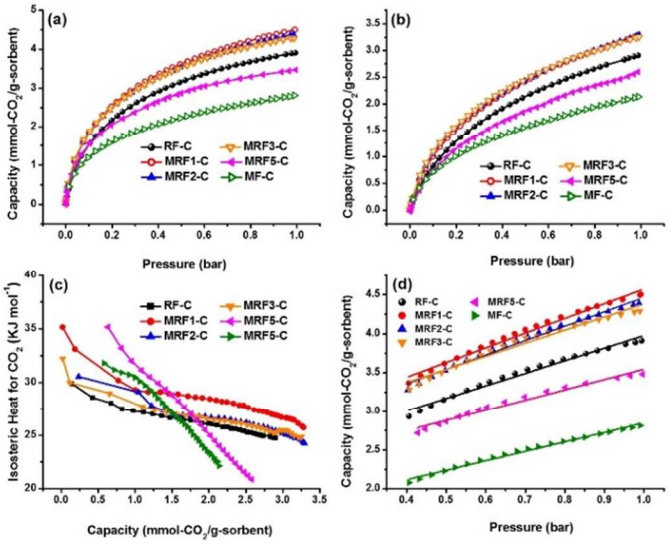

Fig. 7 CO_2 adsorption isotherms at 273 K (a), 298 K (b), the correlation between capacity and pressure on different carbon microspheres at 273 K (c) and isosteric heats of CO2 adsorption (d)

To investigate the CO_2-capture performance of the carbon described at elevated temperatures, we measured adsorption isotherms of MRF1-C at 0, 25, 50, and 75°C. In general, with an increase in adsorption temperature, the adsorption capacities of MRF1-C decrease from 4.50 mmol/g at 0 °C to 1.60 mmol/g at 75 °C. The CO_2 adsorption capacity lies strongly with the balance of kinetic diffusion and thermodynamic adsorption. The temperature-dependent adsorption results suggest that the CO_2 adsorption of MRF1-C is a thermodynamic control process in accordance with the exothermic character of physical adsorption. On the other hand, the decrease in CO_2 capture capacity at high temperatures indicates that carbon microspheres not only can afford high CO_2 capture capacity but also can be regenerated at mild conditions, which is also an important design metric for practical CO_2 adsorbents.

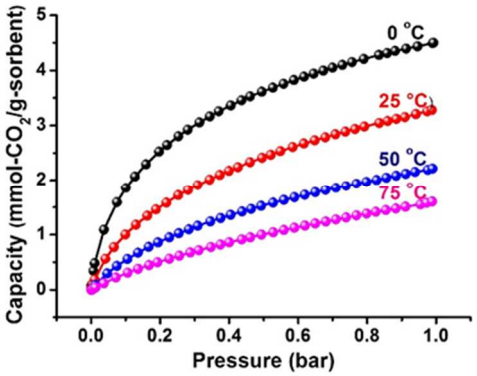

Fig. 8 CO_2 adsorption capacity for MRF1-C at different temperatures

For a cost-effective capture of CO_2, the sorbents should not only possess high adsorption capacity but also have fast adsorption kinetics. Fig. 9a shows the typical adsorption kinetics of CO_2 over MRF1-C at 25 °C conducted on thermogravimetric (TG) analyzer. The CO_2 capture appeared to be a two stage process. Once the sorbents were exposed in the CO_2 stream, a sharp linear weight gain occurred in the first stage, which was completed in less than 10 min followed by a plateau corresponding to a much slower adsorption process. Furthermore, the first stage of adsorption holds as high as 80% of the total capacities. The good kinetics is beneficial in shortening the adsorption cycle time for potential practical applications.

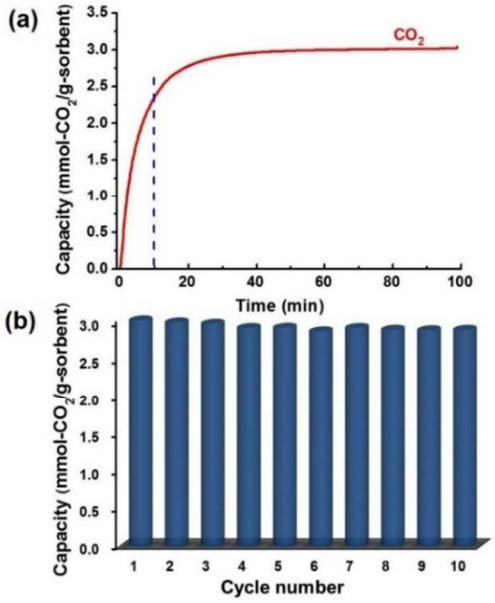

Fig. 9 CO_2 adsorption kinetics for MRF1-C at 25 °C (a) and regeneration performance of MRF1-C at 25 °C (b).

Nitrogen-enriched carbon microspheres have also been analysed under repeated cycles in order to explore the versatility of these materials in a subsequent regeneration step.

Fig. 9b demonstrates the cycling performance of MRF1-C tested on TG analyser at 25 °C. The cyclical data reveals that the performance of the MRF1-C sorbents is fairly stable, with only a 3% drop in the adsorption capacity after 10 cycles. This implies that the MRF1-C can be completely regenerated due to the establishment of moderate interactions between CO_2 molecule and the sorbent. Thus, the MRF1-C can be envisaged as excellent candidates for stable performance in practical cyclic operations such as pressure swing adsorption.

3.3 CO_2 activation

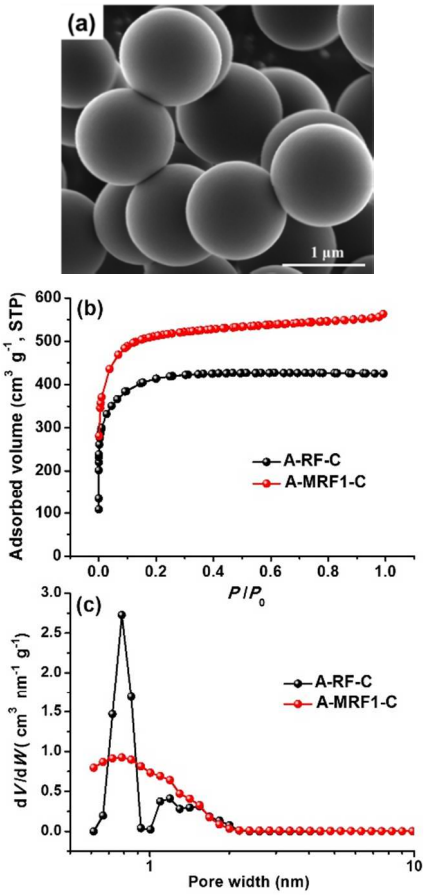

Fig. 10 SEM image (a), N2 adsorption isotherms at 77K (b) and pore size distributions (c) of activated carbon microspheres

Although direct carbonization of MRF microspheres could produce the nitrogen-enriched carbon microspheres with considerable micropores, higher surface area is generally necessary for carbon materials in adsorption and electrochemical applications where micropore plays a dominate role. Here we demonstrate that a simple CO_2 activation of MRF carbon microspheres at 900 °C for 3h could create extremely high micropores into the microspheres. After a mild activation, it can well preserve the spherical morphology but with a little shrinkage compared to the parent carbon microspheres (Fig. 10a). Meanwhile, the nitrogen content of activated carbon A-MRF1-C microspheres can still remain 2.42 wt. % compared to 7.36 wt. % of MRF1-C. The N_2 adsorption-desorption isotherms of the activated carbon microspheres are shown in Fig. 10b. All isotherms are type I with a distinct adsorption plateau at low relative pressure, indicating the presence of highly microporous structure. The specific surface area and pore structure parameters are listed in Table 3. The surface area of the activated carbon microspheres studied range from 1544 to 1952 m^2/g, which indicates about 900-1200 m^2/g enhancement as compared to the respective non-activated carbon microspheres. Obviously, this enlargement in the surface area is due to the creation of additional micropores during CO_2 activation process. It should be noted that, at the some activation conditions, nitrogen-doped carbon microspheres exhibit much higher specific surface area and broader micropore size distribution compared to nitrogen-free carbon microspheres. This is probably due to the presence of more active nitrogen-contained graphitic structure, which can be easily react with CO_2 during activation, leading to the formation of more micropores. The detailed activation mechanism and their potential applications will be discussed in the subsequent paper.

Table 3. Porosity parameters of the carbon microspheres after activation

Samples	S_{BET}[a] (m^2/g)	S_{mic}[b] (m^2/g)	V_{total}[c] (cm^3/g)	V_{mic}[d] (cm^3/g)
A-RF-C	1544	1383	0.66	0.57
A-MRF-1-C	1952	1813	0.87	0.74

4 Conclusion

Nitrogen-enriched carbon microspheres with uniform and monodispersed morphology were synthesized using melamine-resorcinol-formaldehyde as precursors by hydrothermal polymerization and subsequent carbonization. The synthesis is scalable, low cost and flexible, permitting a facile control of particle size, porous structure and nitrogen content by adjusting the precursor molar ratio of melamine to resorcinol. The obtained carbon microspheres have a high BET surface area of 400-800 m^2/g and a controllable nitrogen content of 0-22.5 wt. %. CO_2 capture experiments demonstrated that the carbon microspheres are excellent CO_2 adsorbents with the capacity up to 4.50 mmol/g at 273 K and 3.29 mmol/g at 298 K. This may be due to the coexistence of nitrogen functional groups and abundant micropores. In addition, the carbon microspheres showed fast CO_2 adsorption kinetics, stable performance during long cycles and can be easily regenerated. These features make the synthesized carbon microspheres promising CO_2 adsorbents for practical applications. Moreover, these carbon microspheres can further treated by CO_2 activation to greatly improve their BET surface areas, making them more suitable for various applications.

Acknowledgements

This work was partly supported by MOST (2014CB239702) and National Science Foundation of China (No. 51302083, No. 51172071, No.51272077), and Fundamental Research Funds for the Central Universities and Program of Shanghai Subject Chief Scientist (No 13XD1424900).

Notes and references

[a] State Key Laboratory of Chemical Engineering, East China University of Science and Technology, Shanghai 200237, China..

[b] Key Laboratory of Specially Functional Polymeric Materials and Related Technology, East China University of Science and Technology, Shanghai 200237, China.

*Corresponding author: Donghui Long, Tel: +86 21 64252924, Fax: +86 21 64252914. E-mail: longdh@mail.ecust.edu.cn

† Electronic Supplementary Information (ESI) available: [SEM images and elemental analysis of the as-prepared polymer microspheres]. See DOI: 10.1039/b000000x /

1. X. Sun and Y. Li, *Angew. Chem., Int. Ed*, 2004, **43**, 597.
2. J. Kim, H. S. Kim, N. Lee, T. Kim, H. Kim, T. Yu, I. C. Song, W. K. Moon and T. Hyeon, *Angew. Chem., Int. Ed*, 2008, **47**, 8438.
3. J. Y. Kim, S. B. Yoon and J.-S. Yu, *Chem. Commun.*, 2003, **6**, 790.
4. S.-R. Guo, J.-Y. Gong, P. Jiang, M. Wu, Y. Lu and S.-H. Yu, Adv. *Funct. Mater.*, 2008, **18**, 872.
5. Y. Wang, S. Song, V. Maragou, P. K. Shen and P. Tsiakaras, *Appl. Catal. B: Environ.*, 2009, **89**, 223.
6. Y. Z. Jin, Y. J. Kim, C. Gao, Y. Q. Zhu, A. Huczko, M. Endo and H. W. Kroto, *Carbon*, 2006, **44**, 724.
7. W. Li, D. Chen, Z. Li, Y. Shi, Y. Wan, G. Wang, Z. Jiang and D. Zhao, *Carbon*, 2007, **45**, 1757.
8. N. P. Wickramaratne and M. Jaroniec, *ACS Appl. Mater. Interfaces*, 2013, **5**, 1849.
9. J. Jiang, Q. Gao, Z. Zheng, K. Xia and J. Hu, Int. J. *Hydrogen. Energ.*, 2010, **35**, 210.
10. L. Liu, Q.-F. Deng, X.-X. Hou and Z.-Y. Yuan, *J. Mater. Chem.*, 2012, **22**, 15540.
11. K. Pan, H. Ming, Y. Liu and Z. Kang, *New J. Chem.*, 2012, **36**, 113.
12. M. Li, W. Li and S. Liu, *Carbohydr Res*, 2011, **346**, 999.
13. Y. Mi, W. Hu, Y. Dan and Y. Liu, *Mater. Lett.*, 2008, **62**, 1194.
14. B. Sunkara, J. Zhan, J. He, G. L. McPherson, G. Piringer and V. T. John, *ACS Appl. Mater. Interfaces.*, 2010, **2**, 2854.
15. C. Xu, L. Cheng, P. Shen and Y. Liu, *Electrochem. Commun.*, 2007, **9**, 997.
16. M. Zhang, H. Yang, Y. Liu, X. Sun, D. Zhang and D. Xue, *Carbon*, 2012, **50**, 2155.
17. M. Sevilla and A. B. Fuertes, *Carbon*, 2009, **47**, 2281.
18. X. Cui, M. Antonietti and S.-H. Yu, *Small*, 2006, **2**, 756.
19. T. Horikawa, Y. Ono, J. i. Hayashi and K. Muroyama, *Carbon*, 2004, **42**, 2683.
20. B. Friedel and S. Greulich-Weber, *Small*, 2006, **2**, 859-863.
21. J. Yao, H. Wang, J. Liu, K.-Y. Chan, L. Zhang and N. Xu, *Carbon*, 2005, **43**, 1709.
22. D. Long, R. Zhang, W. Qiao, L. Zhang, X. Liang and L. Ling, *J Colloid Interface Sci*, 2009, **331**, 40.
23. C.-M. Lei, W.-L. Yuan, H.-C. Huang, S.-W. Ho and C.-J. Su, *Synth. Met.*, 2011, **161**, 1590.
24. H.-s. Qian, F.-m. Han, B. Zhang, Y.-c. Guo, J. Yue and B.-x. Peng, *Carbon*, 2004, **42**, 761.
25. V. G. Pol, M. Motiei, A. Gedanken, J. Calderon-Moreno and M. Yoshimura, *Carbon*, 2004, **42**, 111.
26. Y. Yang, X. Liu, C. Y. Zhang, M. Guo and B. Xu, *J. Phys. Chem. Solids.*, 2010, **71**, 235.
27. J. Liu, S. Z. Qiao, H. Liu, J. Chen, A. Orpe, D. Zhao and G. Q. Lu, *Angew. Chem., Int. Ed.*, 2011, **50**, 5947.
28. X. Zhang, Y. Li and C. Cao, *J. Mater. Chem.*, 2012, **22**, 13918.
29. W. Kim, J. B. Joo, N. Kim, S. Oh, P. Kim and J. Yi, *Carbon*, 2009, **47**, 1407.
30. M.-C. Huang and H. Teng, *Carbon*, 2003, **41**, 951.
31. C. Pevida, T. C. Drage and C. E. Snape, *Carbon*, 2008, **46**, 1464.
32. Y.-R. Dong, N. Nishiyama, M. Kodama, Y. Egashira and K. Ueyama, *Carbon*, 2009, **47**, 2138.
33. P.-X. Hou, H. Orikasa, T. Yamazaki, K. Matsuoka, A. Tomita, N. Setoyama, Y. Fukushima and T. Kyotani, *Chem. Mater.*, 2005, **17**, 5187.
34 G.-P. Hao, W.-C. Li, D. Qian and A.-H. Lu, *Adv. Mater.*, 2010, **22**, 853.
35 J. Zhou, W. Li, Z. Zhang, W. Xing and S. Zhuo, *RSC Advances*, 2012, **2**, 161.
36 X. Zhu, P. C. Hillesheim, S. M. Mahurin, C. Wang, C. Tian, S. Brown, H. Luo, G. M. Veith, K. S. Han, E. W. Hagaman, H. Liu and S. Dai, *ChemSusChem*, 2012, **5**, 1912.
37 J. Wang and Q. Liu, *Nanoscale*, 2014, **6**, 4148.
38 J. Wang, I. Senkovska, M. Oschatz, M. R. Lohe, L. Borchardt, A. Heerwig, Q. Liu and S. Kaskel, *J. Mater. Chem. A*, 2013, **1**, 10951.
39 J. Wang, I. Senkovska, M. Oschatz, M. R. Lohe, L. Borchardt, A. Heerwig, Q. Liu and S. Kaskel, *ACS Appl. Mater. Inter.*, 2013, **5**, 3160.
40 J. Wang, A. Heerwig, M. R. Lohe, M. Oschatz, L. Borchardt and S. Kaskel, *J. Mater. Chem.*, 2012, **22**, 13911.
41 J. A. Thote, K. S. Iyer, R. Chatti, N. K. Labhsetwar, R. B. Biniwale, S. S. Rayalu, *Carbon*, 2010, **48**, 396.
42 D. Qian, C. Lei, En. Wang, W. Li, and An. Lu, *ChemSusChem*, 2014, **7**, 291.
43 N. P. Wickramaratne and M. Jaroniec, *ACS Appl. Mater. Interfaces*, 2011, **5**, 1849.
44 V. Presser, J. McDonough, S. H. Yeon and Y. Gogotsi, *Energy Environ. Sci.*, 2011, **4**, 3059.
45 H. Zhou, S. Xu, H. Su, M. Wang, W. Qiao, L. Ling, D. Long, *Chem. Commun.*, 2013, **49**, 3763..
46. V. Presser, J. McDonough, S.-H. Yeon and Y. Gogotsi, *Energy Environ. Sci.*, 2011, **4**, 3059.
47. N. P. Wickramaratne and M. Jaroniec, J. Mater. Chem. A, 2013, 1, 112.
48. J. Li, R. Lu, B. Dou, C. Ma, Q. Hu, Y. Liang, F. Wu, S. Qiao and Z. Hao, *Energy Environ. Sci.*, 2012, **46**, 12648.
49. S. Tao, Y. Wang, D. Shi, Y. An, J. Qiu, Y. Zhao, Y. Cao and X. Zhang, *J. Mater. Chem. A*, 2014, **2**, 12785.
50. C. Chen, J. Kim and W.-S. Ahn, *Fuel*, 2012, **95**, 360.
51. C. Pevida, T.C. Drage and C.E. Snape, *Carbon*, 2008, **46**, 1464.
52. N. P. Wickramaratne, J. Xu, M. Wang, L. Zhu, L. Dai and M. Jaroniec, *Chem. Mater.*, 2014, **26**, 2820.

53. M.S. Shafeeyan, W. M. A. W. Daud, A. Houshmand and A. Arami-Niya, *Appl. Surf. Sci.*, 2011, **257**, 3936.
54. J. Wei, D. Zhou, Z. Sun, Y. Deng, Y. Xia and D. Zhao, *Adv. Funct. Mater.*, 2013, **23**, 2322
55. K. Chue, J. Kim, Y. Yoo, S. Cho and R. Yang, *Ind. Eng. Chem. Res.*, 1995, **34**, 591.
56. B. Arstad, H. Fjellvåg, K. O. Kongshaug, O. Swang and R. Blom, *Adsorption*, 2008, **14**, 755.

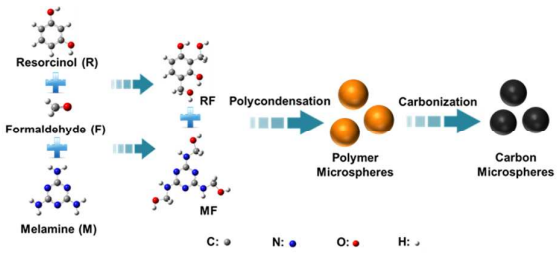

Nitrogen-enriched carbon microspheres with uniform and monodispersed morphology can be synthesized *via* a facile, scalable and environmental friendly process.